Title: CHK1 inhibition in small cell lung cancer produces single-agent activity in biomarker-defined disease subsets and combination activity with cisplatin or olaparib

Authors: Triparna Sen[1], Pan Tong[2], C. Allison Stewart[1], Sandra Cristea[3,4], Aly Valliani[1], David S. Shames[5], Abena B. Redwood[6], You Hong Fan[1], Lerong Li[2], Bonnie S. Glisson[1], John D. Minna[7], Julien Sage[3,4], Don L. Gibbons[1,8], Helen Piwnica-Worms[6], John V. Heymach[1,9], Jing Wang[2], and Lauren Averett Byers[1]*

Affiliations: [1]Departments of [1]Thoracic/Head and Neck Medical Oncology, [2]Bioinformatics and Computational Biology, [6]Experimental Radiation Oncology, [8]Molecular and Cellular Oncology and [9]Cancer Biology, The University of Texas MD Anderson Cancer Center, Houston, TX 77030, USA. Departments of [3]Pediatrics and [4]Genetics, Stanford University, Stanford, CA 94305, USA; [5]Department of Oncology Biomarker Development, Genentech Inc., South San Francisco, CA 94080, USA; [7]Hamon Center for Therapeutic Oncology Research, The University of Texas Southwestern, Dallas, TX 75390, USA

*To whom correspondence should be addressed: lbyers@mdanderson.org

Supplementary Figure and Figure Legends

Figure S1

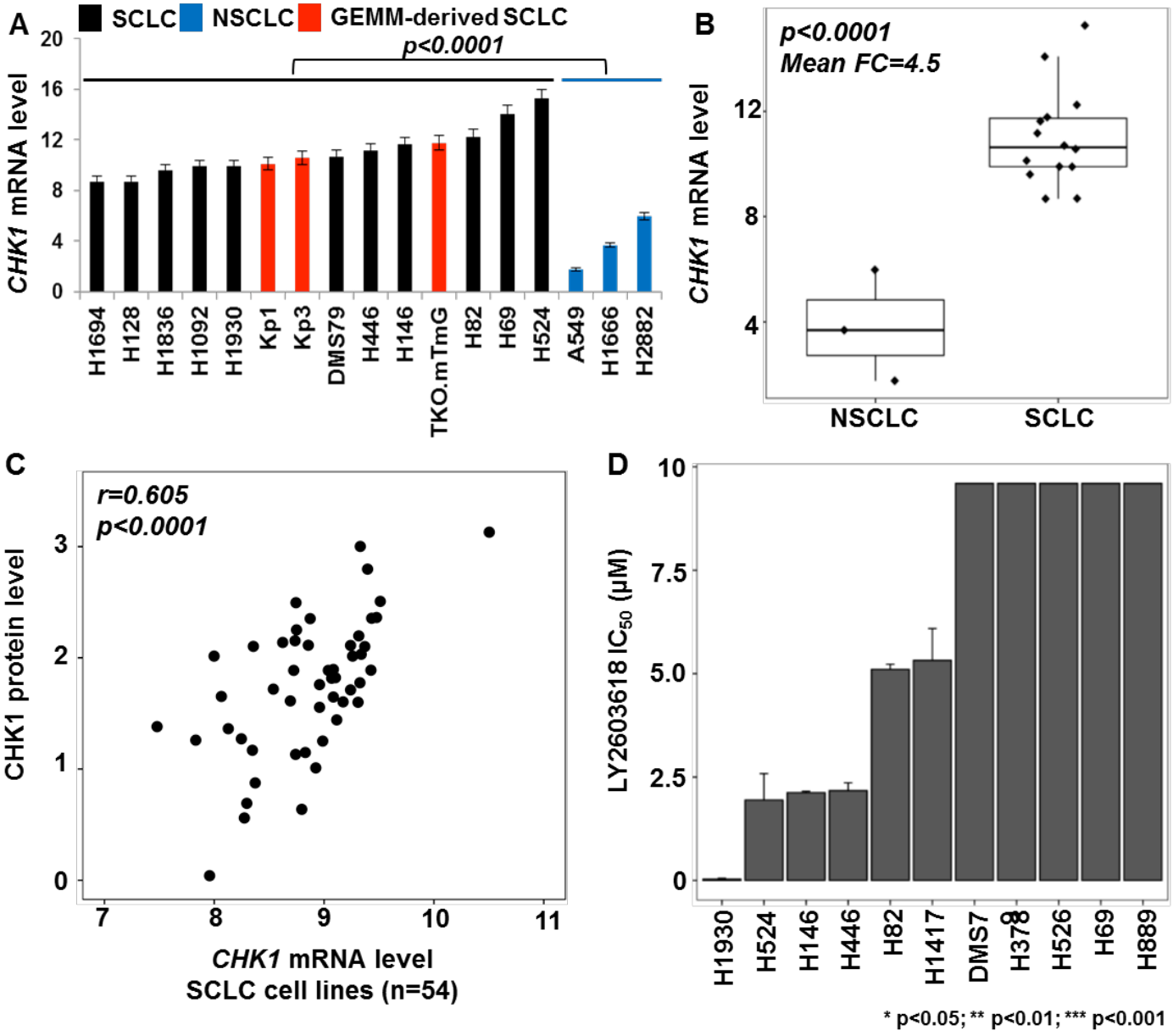

Figure S1. *CHK1* is overexpressed in small cell lung cancer (SCLC) cell lines, and targeting CHK1 with LY2603618 decreases the viability of human SCLC cell lines.

(A) Quantitative polymerase chain reaction was used to detect expression of *CHK1* in human (n = 11) and genetically engineered mouse model (GEMM)-derived (n = 3) SCLC cell lines (Kp1,

Kp3, and TKO.mTmG: *Rb*;*p53*;*p130* knockout) and human non-small cell lung cancer (NSCLC) cell lines (n = 3). Target gene expression is normalized to *GAPDH* expression. Data are presented as mean ± standard error of the mean (error bars) of three independent experiments. (B) Comparative t-test of the mean mRNA expression of *CHK1* as shown in Figure S1A between NSCLC (n=3) and SCLC (n=11) cell lines ($p<0.0001$; Mean FC=4.5). **$p < 0.01$; ***$p < 0.001$. Genetic profile information of the cell lines is presented in **Table S1.** (C) Pearson correlation demonstrates positive correlation between CHK1 protein and mRNA expression in SCLC cell lines (n=54) ($r=0.605$; $p<0.0001$). (D) Sensitivity of a subset of SCLC cell lines (n = 11) to a second CHK1 inhibitor, LY2603618, as measured by a 7-day CellTiter-Glo analysis. For single-agent analysis, the half-maximal inhibitory concentration (IC_{50}) value was estimated using drexplorer software, which fitted multiple dose-response models and selected the best model using residual standard.

Figure S2

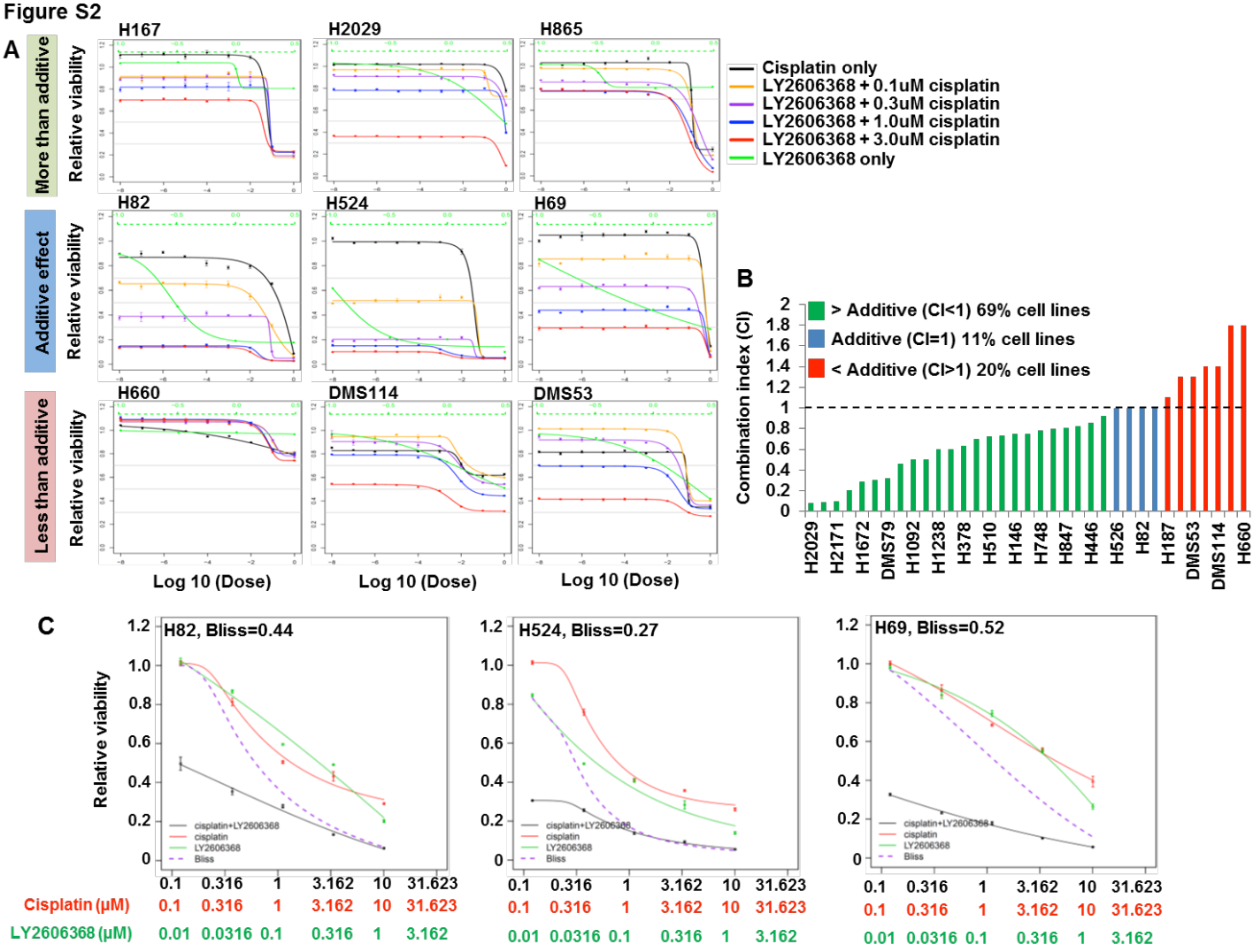

Figure S2. Treatment with LY2606368 potentiates the cytotoxic effect of cisplatin in small cell lung cancer (SCLC) cell lines. (A) Dose-response curves showing the effect of increasing doses of LY26063638 in combination with fixed doses of cisplatin (0.1, 0.3, 1, or 3μM) on cell viability in SCLC cell lines. For drug combination analysis, we used MacSynergy II (http://www.uab.edu/medicine/peds/macsynergy) to calculate metrics, including synergistic volume, antagonistic volume, overall volume, and extra kill percentage. (B) Combination index of LY2606368 and cisplatin across 35 human SCLC cell lines demonstrating that LY2606368 great augments the cytotoxic effect of cisplatin in majority of SCLC cell lines (green bars; n=24).

(C) Dose-response curve of three human SCLC cell lines (H82, H69, H524) treated with clinically relevant doses of cisplatin (10-0.1μM) (red), LY2606368 (green), and cisplatin+LY2606368 (black), from a 5-day cell titer Glo assay.

Figure S3

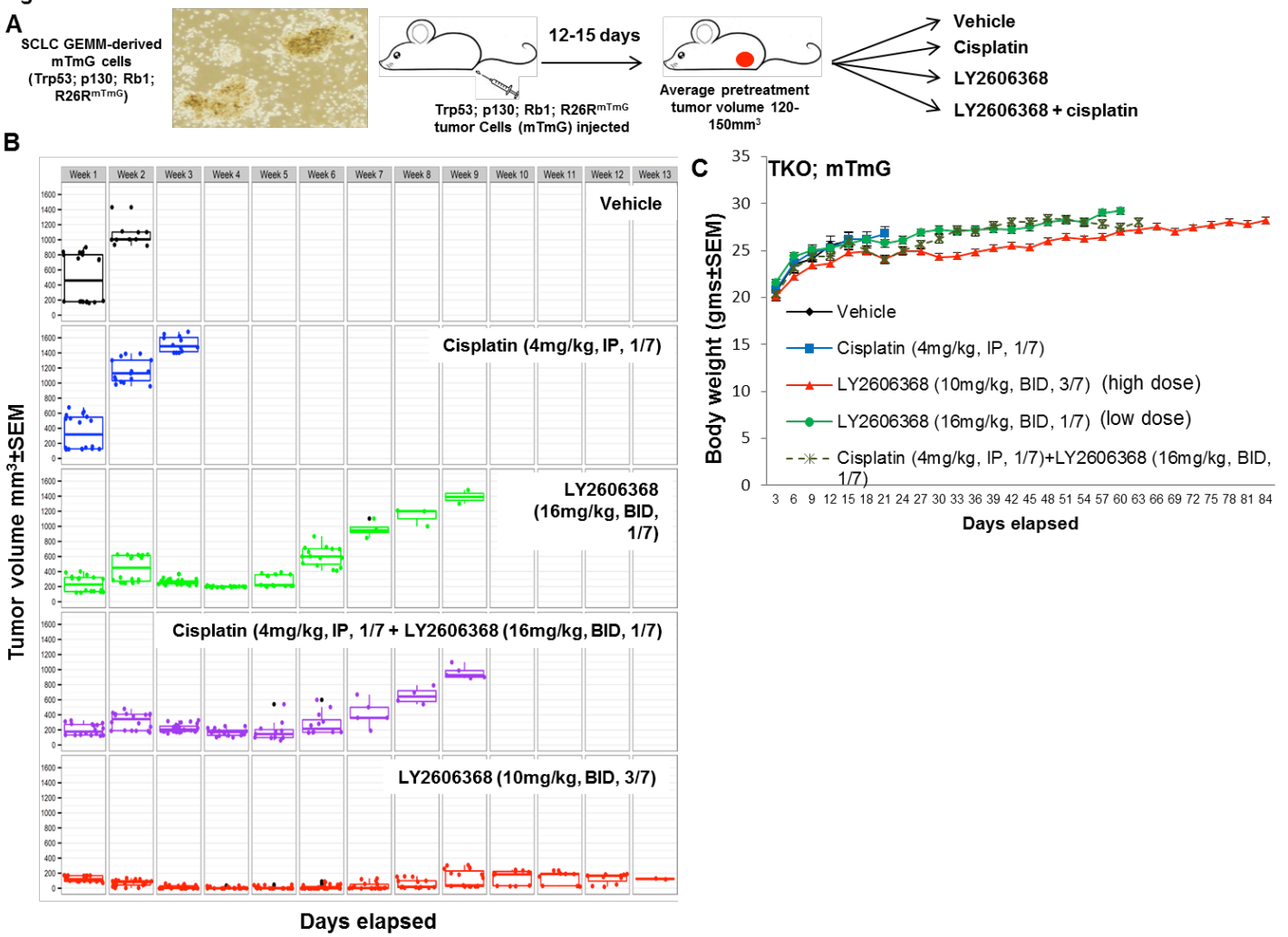

Figure S3. CHK1 inhibition, alone or in combination with cisplatin, causes significant tumor regression in a syngeneic model of small cell lung cancer (SCLC). (A) Schematic overview of treatment with vehicle (control), LY2606368, or cisplatin + LY2606368 in a flank xenograft model of SCLC. Single-agent LY2606368 was administered at a dose of 10 mg/kg twice, daily, three times per week (60 mg/kg per week; high dose) or 16 mg/kg, twice daily, once per week (32 mg/kg per week; low dose). Single-agent cisplatin was administered at a dose of 4 mg/kg, once per week. Cisplatin + LY2606368 were administered as follows: cisplatin 4 mg/kg, once per week, day 1 of a 7-day cycle; LY2606368 16 mg/kg, twice daily, once per week, day 2

of a 7-day cycle. (B) Box plots showing the change in absolute tumor volume of individual animals in each group throughout the treatment schedule, by week. These data demonstrate significant antitumor efficacy of high-dose single-agent LY2606368 and the cisplatin + LY2606368 combination. (C) Body weight of mice measured three times per week after treatment was started. No noticeable weight loss was observed with either the single-agent or combination schedules. Error bars indicate SEM.

Figure S4

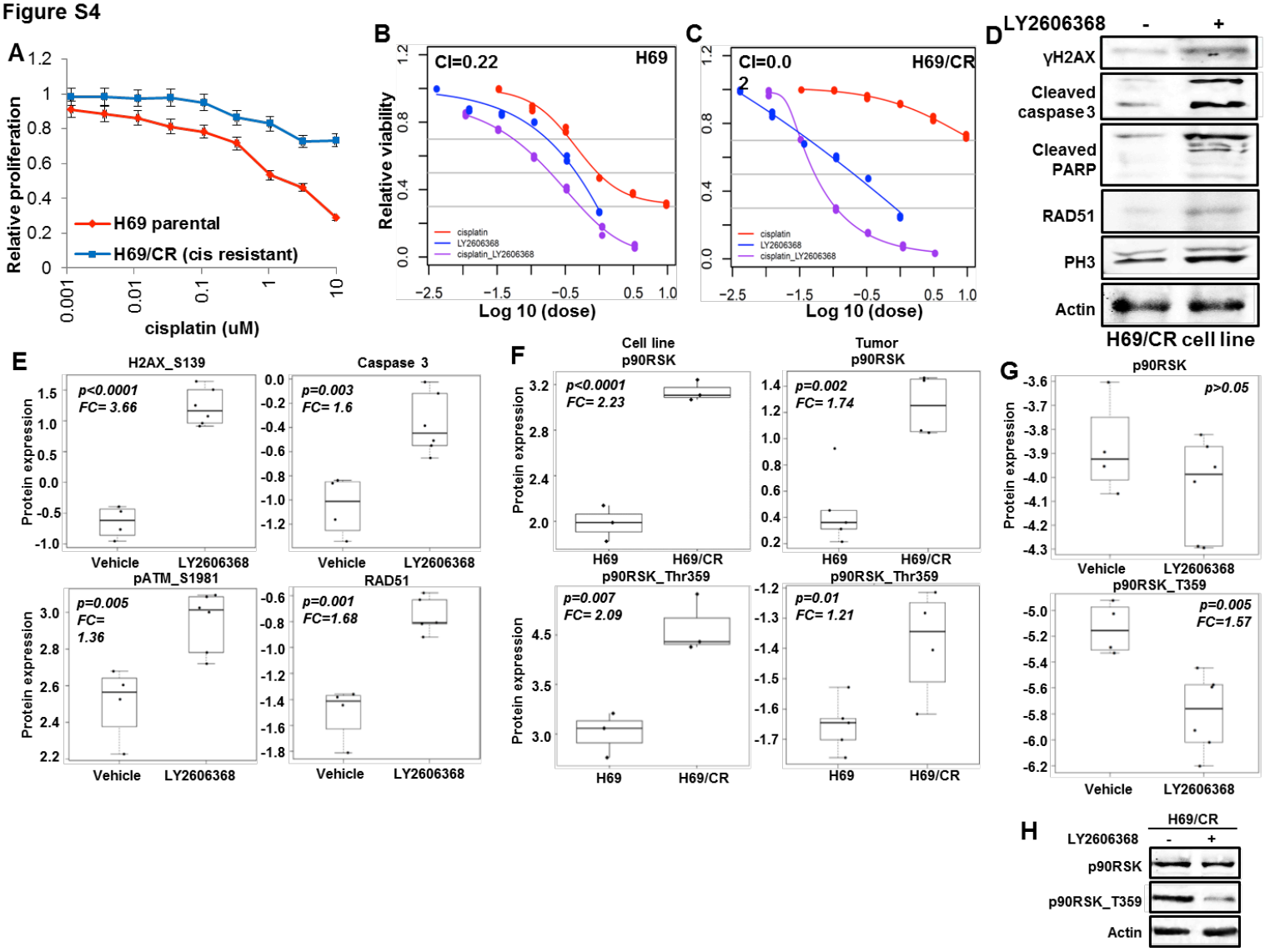

Figure S4. Platinum-resistant models of small cell lung cancer (SCLC) are sensitive to the CHK1 inhibitor LY2606368. (A) To prove cisplatin resistance, we treated human SCLC cell lines H69 (parental cisplatin resistance) and H69/CR (acquired cisplatin resistance) with increasing concentrations of cisplatin. The effect of cisplatin was measured by cell viability assay. The separation of the lines on the graph demonstrates the cisplatin resistance in H69/CR cells. (B and C) Chemosensitive H69 (B) and chemoresistant H69/CR (C) cells were treated with single-agent LY2606368 and cisplatin or the combination of the drugs. Cell viability was

measured by a 7-day CellTiter-Glo assay. Data represent means ± standard error of the mean (error bars) of three independent experiments. The combination index (CI) at fraction affected (FA) = 0.5 was 0.22 for H69 and 0.02 for H69/CR, as calculated by the Loewe model. (D) Western blot analysis of H69/CR cell lines treated with or without LY2606368 (30nM, 24 hours) shows increased γH2AX, cleaved caspase 3, cleaved PARP, RAD51 and PH3 post-LY2606368 treatment. Actin was used as loading control. (E) Box plots of proteins expression measured by RPPA demonstrate higher γH2AX, caspase 3, pATM_S1981 and RAD51 post-LY2606368 treatment in H69/CR tumor models. (F) Box plots of proteins expression measured by RPPA demonstrate higher total and phospho p90RSK_Thr359 level in chemo-resistant H69/CR cell line and tumor models as compared to parental chemo-sensitive H69 models. (G) Box plots of proteins expression measured by RPPA demonstrate significantly lower phospho p90RSK_Thr359 level post-LY2606368 treatment in H69/CR tumor models. (H) Western blot analysis in H69/CR cell lines treated with or without LY2606368 treatment showed lower phospho p90RSK_Thr359 level post-LY2606368 treatment in H69/CR cell line.

Figure S5

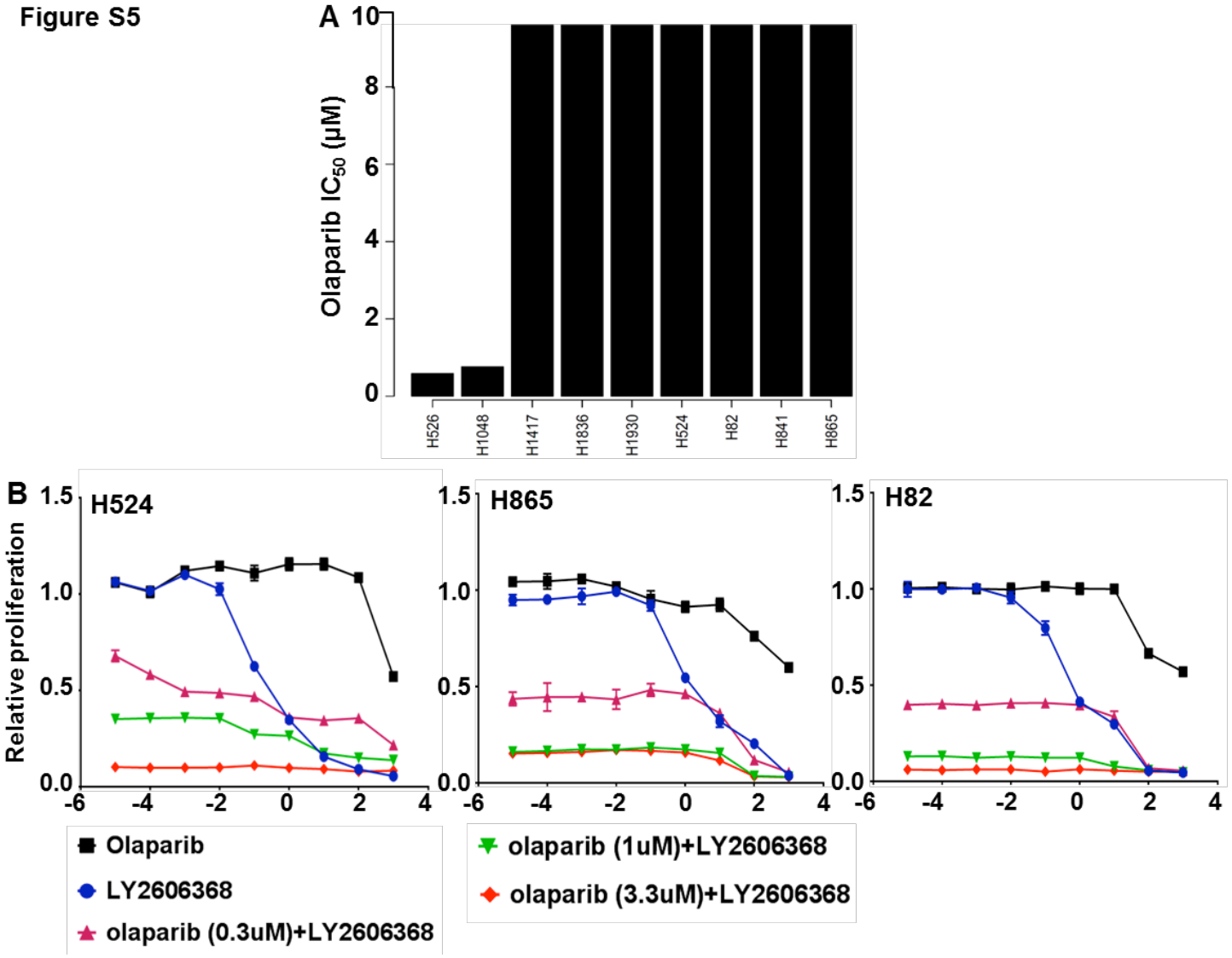

Figure S5. CHK1 and PARP inhibitors synergistically decrease viability in small cell lung cancer (SCLC) models. (A) Cell viability in response to treatment with single-agent olaparib in a panel of human SCLC cell lines (n = 9). The genetic profile information for each cell line is presented in Table S1. (B) Three SCLC cell lines (H524, H82, H865) showing *de novo* resistance to single-agent olaparib after exposure to increasing doses of LY26063638 in combination with fixed doses of olaparib (0.3, 1, or 3μM). Dose-response curves show the effect of the drug combination on cell viability at different doses.

Figure S6

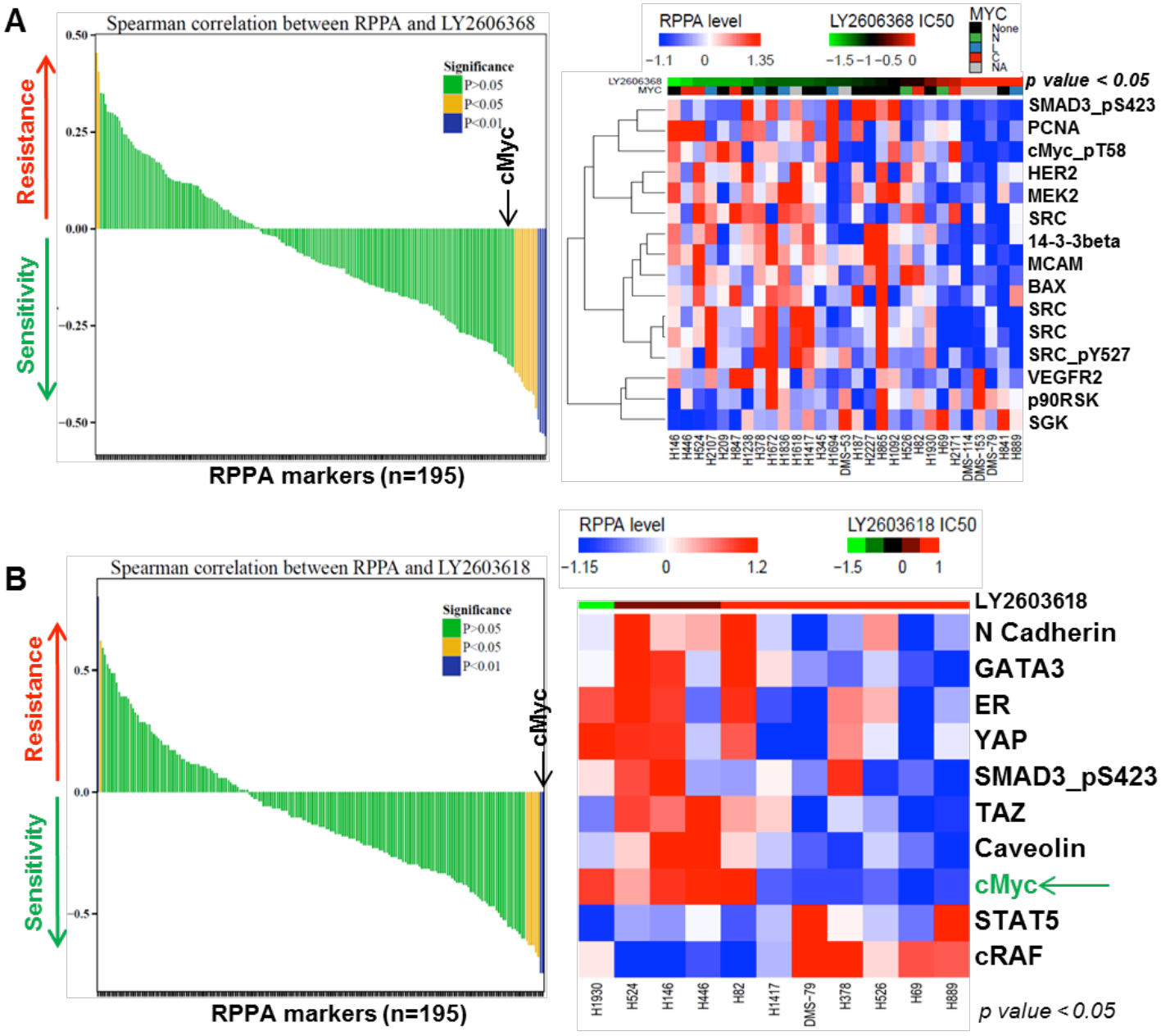

Figure S6. Proteomic analysis identifies biomarkers that predict response to CHK1 inhibition. (Left panels) Spearman correlation between proteomic profiles of small cell lung cancer (SCLC) cell lines as determined by an analysis of 195 reverse-phase protein array (RPPA) markers and sensitivity to LY2606368 (A) and LY2603618 (B). (Right panels) Heat map of

RPPA markers significantly associated with LY2606368 (A) and LY2603618 (B) response in human SCLC cell lines ($p < 0.05$). In the top index, cell lines with relatively low LY2606368 half-maximal inhibitory concentration (IC_{50}) values are marked in green and those with relatively high IC_{50} values are marked in red. The cell lines are grouped according to their MYC status and marked as having no MYC amplification (black), *MYCN* amplification (green), *MYCL* amplification (blue), *MYC* amplification (red), and unknown amplification (gray).

Figure S7

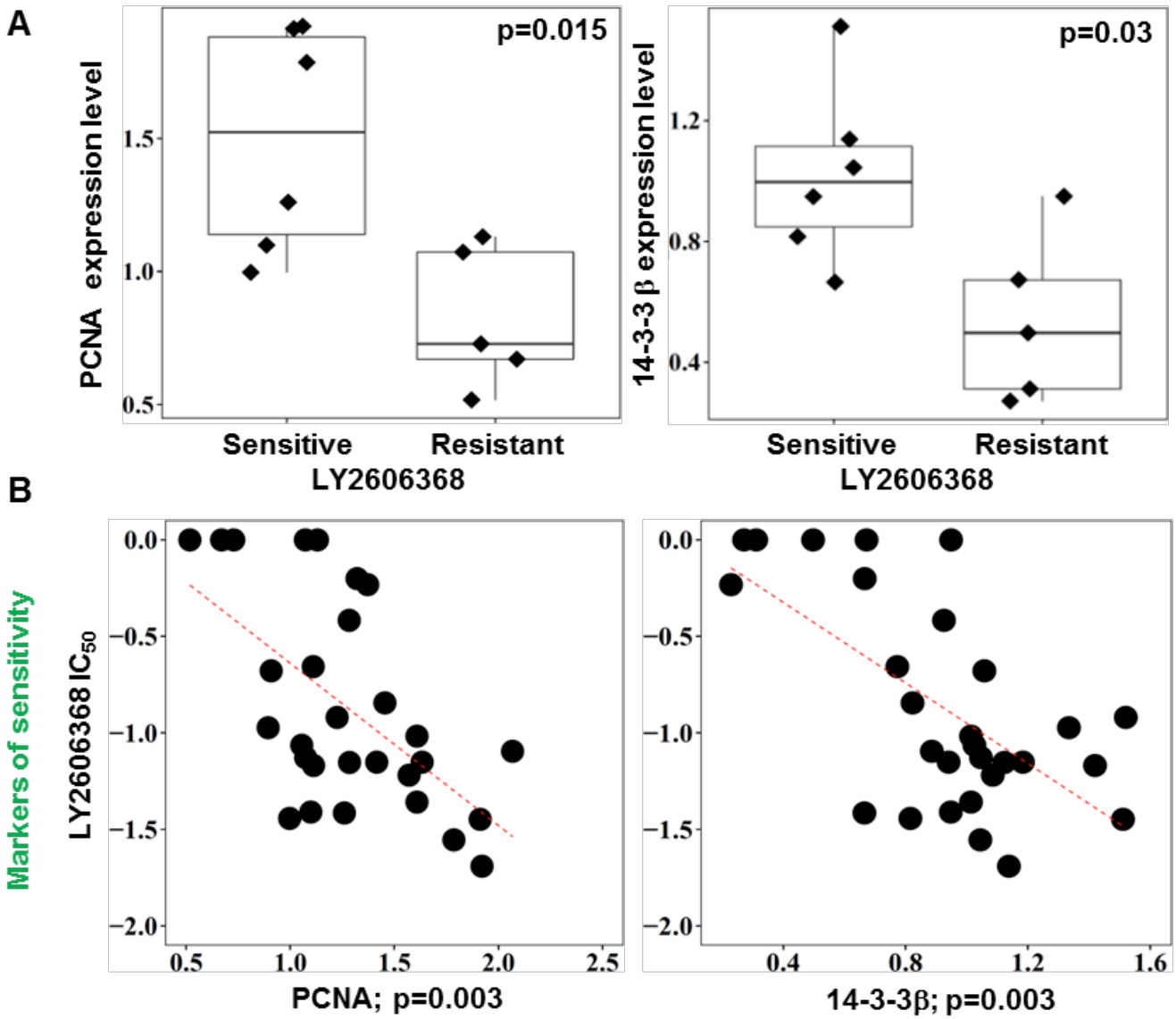

Figure S7: Additional biomarkers were associated with sensitivity to CHK1 inhibition in small cell lung cancer. (A) Box plots of additional reverse-phase protein array (RPPA) markers significantly correlated with dichotomized half-maximal inhibitory concentrations (IC_{50}) of LY2606368 as determined by *t* test. The top markers of sensitivity to CHK1 inhibition in this set were PCNA (p = 0.015) and 14-3-3β (p = 0.03). (B) Scatter plots of individual RPPA markers

associated with sensitivity to LY2606368. The p values of the top markers of sensitivity—PCNA ($p = 0.003$) and 14-3-3β ($p = 0.003$)—were determined by Spearman correlation.

Figure S8

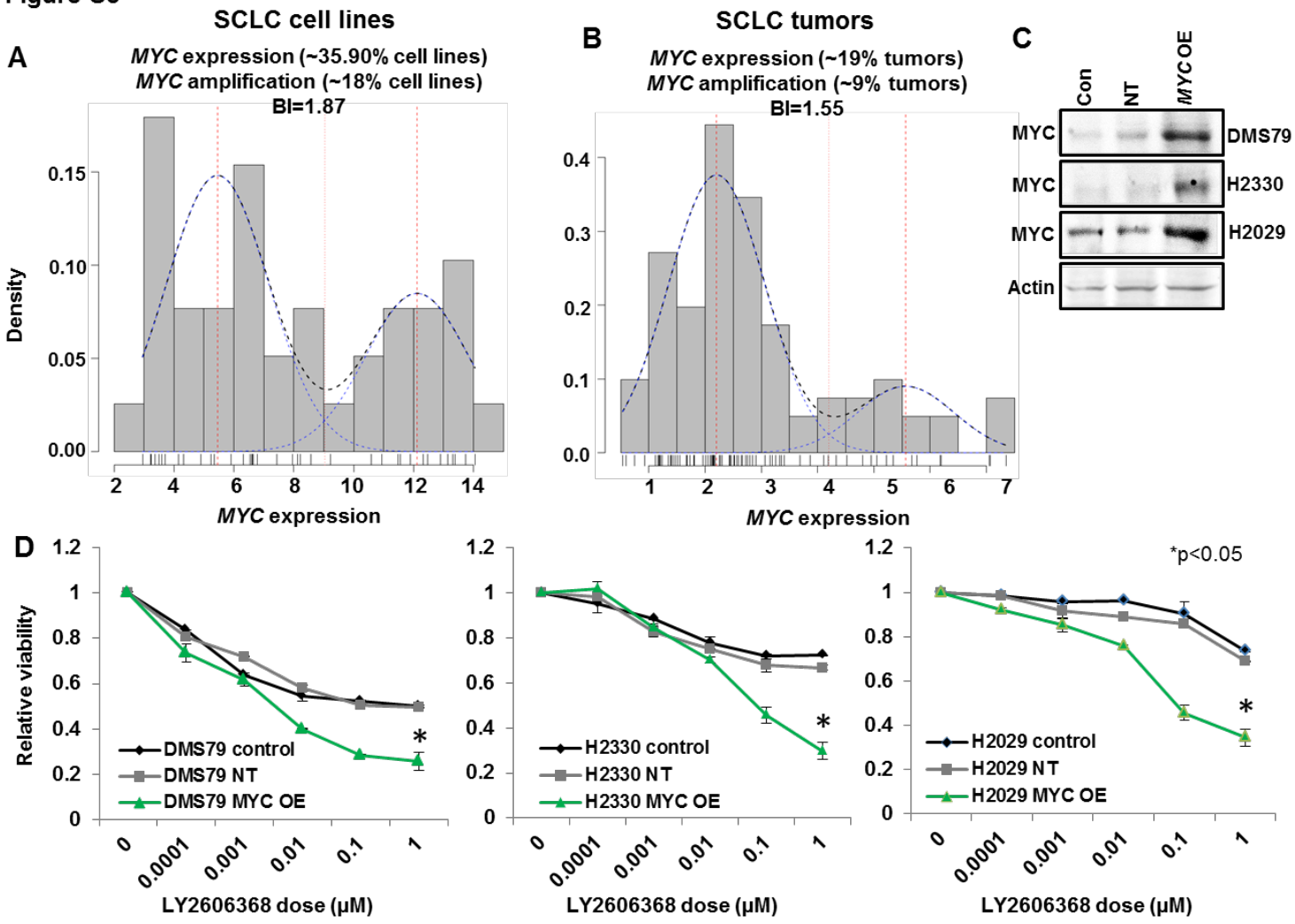

Figure S8: *MYC* expression represents a larger subset of SCLC patient and cell lines as compared to *MYC* amplification alone and overexpression of *MYC* sensitizes SCLC cells to LY2606368 treatment. (A) and (B) Bimodal distribution of *MYC* expression in SCLC cell lines (A) and patient tumor samples (B). *MYC* expression was observed in 35.9% SCLC cell lines as compared to *MYC* amplification in only 18% cases (A). Similarly, *MYC* expression in SCLC tumors was 19% as compared to *MYC* amplification in only 9% of tumors (B). (C) Western blot analysis of MYC expression in three cell lines (DMS79, H2029, H2330) to confirm MYC

overexpression (MYC OE) as compared to controls (NT). (D) Dose response curves of three SCLC cell lines show increased sensitivity to LY2606368 treatment post *MYC* overexpression (green) as compared to non-transduced controls.

Title: CHK1 inhibition in small cell lung cancer produces single-agent activity in biomarker-defined disease subsets and combination activity with cisplatin or olaparib

Authors: Triparna Sen[1], Pan Tong[2], C. Allison Stewart[1], Sandra Cristea[3,4], Aly Valliani[1], David S. Shames[5], Abena B. Redwood[6], You Hong Fan[1], Lerong Li[2], Bonnie S. Glisson[1], John D. Minna[7], Julien Sage[3,4], Don L. Gibbons[1,8], Helen Piwnica-Worms[6], John V. Heymach[1,9], Jing Wang[2], and Lauren Averett Byers[1]*

Affiliations: [1]Departments of [1]Thoracic/Head and Neck Medical Oncology, [2]Bioinformatics and Computational Biology, [6]Experimental Radiation Oncology, [8]Molecular and Cellular Oncology and [9]Cancer Biology, The University of Texas MD Anderson Cancer Center, Houston, TX 77030, USA. Departments of [3]Pediatrics and [4]Genetics, Stanford University, Stanford, CA 94305, USA; [5]Department of Oncology Biomarker Development, Genentech Inc., South San Francisco, CA 94080, USA; [7]Hamon Center for Therapeutic Oncology Research, The University of Texas Southwestern, Dallas, TX 75390, USA

*To whom correspondence should be addressed: lbyers@mdanderson.org

Table S1: The genotypic status of human SCLC cell lines and their sensitivity to LY2606368

Cell Line	IC50 of LY2606368 (uM)	*MYCL* Copy Number (qPCR)	*cMYC* Copy Number (qPCR)	*MYCN* Copy Number (qPCR)	TP53 Mutation	*RB1* Status (qPCR)
H146	0.020	No Amp	No Amp	No Amp	Yes	loss
H446	0.027	No Amp	Amp	No Amp	Yes	loss
H524	0.035	No Amp	Amp	No Amp	Yes	loss
H2107	0.036	Amp	No Amp	No Amp	Yes	loss
H209	0.038	No Amp	No Amp	No Amp	Yes	loss
H847	0.039	No Amp	Amp	No Amp	Yes	-
H1238	0.043	No Amp	No Amp	No Amp	Yes	-
H378	0.060	Amp	No Amp	No Amp	Yes	WT
H1672	0.067	No Amp	No Amp	No Amp	Yes	WT
H1836	0.070	Amp	No Amp	No Amp	-	-
H1618	0.070	-	-	-	Yes	loss
H1417	0.070	No Amp	No Amp	No Amp	Yes	loss
H345	0.074	No Amp	No Amp	No Amp	Yes	WT
H1694	0.080	Amp	No Amp	No Amp	Yes	WT
H510	0.080	Amp	No Amp	No Amp	Yes	-
DMS53	0.086	-	-	-	Yes	WT
H187	0.096	No Amp	No Amp	No Amp	Yes	WT
H2227	0.106	No Amp	No Amp	No Amp	Yes	loss
H865	0.120	No Amp	No Amp	No Amp	Yes	-
H1092	0.143	No Amp	No Amp	No Amp	Yes	WT
H719	0.145	No Amp	No Amp	No Amp	Yes	loss
H748	0.146	No Amp	No Amp	No Amp	Yes	loss
H526	0.209	No Amp	No Amp	Amp	Yes	loss
H82	0.221	No Amp	Amp	No Amp	Yes	loss
H1930	0.384	No Amp	No Amp	No Amp	Yes	WT
H69	0.587	No Amp	No Amp	Amp	Yes	loss
H2171	0.631	No Amp	Amp	No Amp	Yes	loss
DMS79	0.878	No Amp	No Amp	No Amp	Yes	loss
DMS153	1	-	-	-	Yes	loss
H889	1	Amp	No Amp	No Amp	Yes	WT
DMS114	1	-	-	-	Yes	WT
H2029	1	No Amp	No Amp	No Amp	Yes	loss
H841	1	No Amp	No Amp	No Amp	Yes	-
H660	1	No Amp	No Amp	No Amp	-	-
H2330	1	No Amp	No Amp	No Amp	-	-

- Denotes data not available

Amp = Amplification; WT= wild type

Table S2: Pairwise p-value of the syngeneic SCLC *in vivo* survival data of Figure 3

Treatment Group 1	Treatment group 2	Pairwise p value
Vehicle	Cisplatin (4mg/kg, IP, 1/7)	**0.0027**
Vehicle	LY2606368 (10mg/kg, BID, 3/7)	**1.3×10^{-5}**
Vehicle	LY2606368 (16mg/kg, BID, 1/7)	**1.3×10^{-5}**
Vehicle	Cisplatin (4mg/kg, IP, 1/7)+ LY2606368 (16mg/kg, BID, 1/7)	**1.3×10^{-5}**
Cisplatin (4mg/kg, IP, 1/7)	LY2606368 (10mg/kg, BID, 3/7)	**5.2×10^{-5}**
Cisplatin (4mg/kg, IP, 1/7)	LY2606368 (16mg/kg, BID, 1/7)	**5.2×10^{-5}**
Cisplatin (4mg/kg, IP, 1/7)	Cisplatin (4mg/kg, IP, 1/7)+ LY2606368 (16mg/kg, BID, 1/7)	**5.2×10^{-5}**
LY2606368 (10mg/kg, BID, 3/7)	LY2606368 (16mg/kg, BID, 1/7)	**0.00043**
LY2606368 (10mg/kg, BID, 3/7)	Cisplatin (4mg/kg, IP, 1/7)+ LY2606368 (16mg/kg, BID, 1/7)	**0.00082**
LY2606368 (16mg/kg, BID, 1/7)	Cisplatin (4mg/kg, IP, 1/7)+ LY2606368 (16mg/kg, BID, 1/7)	**0.72**

Table S3: Primers sequence for *CHEK1 and GAPDH*

Gene	Sense	Antisense	Tm
CHK1	ATA TGA AGC GTG CCG TAG ACT	TGC CTA TGT CTG GCT CTA TTC TG	60°C
GAPDH	AGG GGA GAT TCA GTG TGG TG	GGC CTC CAA GGA GTA AGA CC	63°C

Title: CHK1 inhibition in small cell lung cancer produces single-agent activity in biomarker-defined disease subsets and combination activity with cisplatin or olaparib

Authors: Triparna Sen[1], Pan Tong[2], C. Allison Stewart[1], Sandra Cristea[3,4], Aly Valliani[1], David S. Shames[5], Abena B. Redwood[6], You Hong Fan[1], Lerong Li[2], Bonnie S. Glisson[1], John D. Minna[7], Julien Sage[3,4], Don L. Gibbons[1,8], Helen Piwnica-Worms[6], John V. Heymach[1,9], Jing Wang[2], and Lauren Averett Byers[1]*

Affiliations: [1]Departments of [1]Thoracic/Head and Neck Medical Oncology, [2]Bioinformatics and Computational Biology, [6]Experimental Radiation Oncology, [8]Molecular and Cellular Oncology and [9]Cancer Biology, The University of Texas MD Anderson Cancer Center, Houston, TX 77030, USA. Departments of [3]Pediatrics and [4]Genetics, Stanford University, Stanford, CA 94305, USA; [5]Department of Oncology Biomarker Development, Genentech Inc., South San Francisco, CA 94080, USA; [7]Hamon Center for Therapeutic Oncology Research, The University of Texas Southwestern, Dallas, TX 75390, USA

*To whom correspondence should be addressed: lbyers@mdanderson.org

Supplementary Materials and Methods

Cell culture

Cell lines were grown in RPMI, unless otherwise mentioned by the provider (1), with 10% fetal bovine serum and antibiotics, cultured at 37°C in a humidified chamber with 5% CO_2. All cell lines included in the study were profiled at passage 4-8 to abrogate the heterogeneity introduced by long-term culture. All cell lines were tested for *Mycoplasma* as previously described (2) and the characteristic phenotype (floating aggregates and colony formation) of small cell lung cancer (SCLC) cell lines. We included in the panel three primary mouse SCLC cell lines established from tumors resected from the syngeneic genetically engineered mouse model-derived triple-knockout model of SCLC, which closely mimics the human disease and has a *Trp53f/f, Rb12f/f, Rb1f/f* ($p53^{-/-}$/$p130^{-/-}$/$Rb1^{-/-}$) allelic genotype (3,4).

DNA fingerprinting to confirm cell line identity

DNA was isolated using a QIAamp DNA mini kit from 5-6 x 10^6 cells was isolated (Qiagen, Valencia, CA) following the manufacturer's protocol. The isolated DNA was eluted in elution buffer (100μl) (Buffer AE, Qiagen). The concentration of the DNA and it purity was measured by Nanodrop. Cell line authentication was done by using DNA (50ng) for DNA fingerprint analysis of short tandem repeat profiling (PowerPlex 1.2, Promega, Madison, WI). Fingerprinting results for each cell line were compared to reference fingerprints provided by Dr. Minna or the ATCC (1).

Targeted knockdown of *CHK1*

CHK1 shRNA constructs were obtained from GE Dharmacon and transfected into SCLC cell lines according to the manufacturer's instructions.

Knockdown and overexpression of *MYC*

SCLC cells were transfected with Validated Stealth Select RNAi siRNA MYC duplexes at a concentration of 10 nmol/L in Opti-MEM, or with Stealth RNAi Negative Universal Control using Lipofectamine 2000 (all from Invitrogen) according to the manufacturer's protocol. Seventy-two hours after transfection, the cells were subjected to drug treatments. For the cell viability assay, control (scramble) or target knockdown cells were plated in triplicate and treated with LY2606368 at increasing concentrations, after which cell viability was measured by a 5-day cell titer Glo assay. The efficiency of the knockdown in all cases was confirmed by real-time reverse transcriptase PCR and Western blot analysis.

For *MYC* overexpression SCLC cells were transduced with MYC overexpression vector (# OHS5900-202620398) (Dharmacon) according to manufacturer's protocol.

RNA isolation

RNA was isolated using the Direct-zol RNA MiniPrep Kit (Zymo Research, cat# R2050) according to the manufacturer's instructions. RNA concentrations were determined using a NanoDrop 2000 UV-Vis spectrophotometer (Thermo Scientific).

Reverse transcription

Reverse transcription reactions were carried out using SuperScript III First-Strand Synthesis SuperMix (Invitrogen, cat# 18080-400) according to the manufacturer's instructions.

Real-time polymerase chain reaction (PCR)

Real-time PCR was done using SYBR Select Master Mix (Life Technologies, cat# 4472908) according to the manufacturer's protocol. The primers were purchased from Sigma (USA); the details of the primers are given in Table S3. Triplicate PCR reactions were run on ABI (7500 Fast Real Time PCR System) according to the manufacturer's instructions. The comparative Ct method using the average $2\Delta\Delta CT$ value for each set of triplicates was used, and the average of

the biological replicates was calculated. Negative controls were included for every primer set, and GAPDH was used as the positive control.

Cell viability assay

SCLC cell lines were incubated with dimethyl sulfoxide (vehicle control), cisplatin, or LY2606368 for 120 hours at nine distinct concentrations, with the maximum dose being 10μM for cisplatin and 1μM for LY2606268. For the combination, cells were treated with cisplatin (3.1, 1, 0.3, and 0.1μM) 24 hours after plating and with LY2606368 at increasing doses (10^{-8} × 1μM) 24 hours after treatment with cisplatin. A CellTiter-Glo luminescent cell viability assay (Promega) was performed after 120 hours of treatment with LY2606368 as per the manufacturer's specifications. For both assays, six replicates were tested at each concentration, and each test was completed at least twice on different days.

Cell cycle analysis and apoptosis assay by flow cytometry

Cells were pretreated with cisplatin (100nM) and then LY2606368 (10nM) was added and incubated for cell cycle analysis (24 hours) and apoptosis assay (48 hours). Cells were harvested, washed with phosphate-buffered saline, and broken into clumps using trypsin. Cells were then fixed overnight with 70% ethanol. The fixed cells were stained with 25 μg/ml propidium iodide (Sigma) in the presence of 1 μg/ml RNase (Sigma). For the apoptosis assay, cells were seeded at 1.5 × 105 cells/ml in the presence or absence of the drugs. The annexin V–propidium iodide binding assay, using the annexin V–fluorescein isothiocyanate (FITC) Apoptosis Detection Kit (BD Biosciences), was used to evaluate apoptosis, according to the manufacturer's instructions.

Apoptosis of SCLC cells in the presence or absence of CHK1 inhibitor with or without cisplatin was measured as follows. Apoptosis was determined by annexin V binding. For fluorescence-activated cell sorting analysis, data were collected using the Gallios LSRII flow

cytometer (Beckman-Coulter) and analyzed using the Kaluza software. The cell cycle distribution was evaluated by counting more than 10,000 cells per sample.

Preparation of protein lysates

Protein lysate was collected from sub confluent cultures after 24-hr in full-serum media (10% fetal bovine serum [FBS]), serum-starved media (0% FBS), or serum-stimulated media (24 hr of 0% FBS followed by 30 min of 10% FBS immediately before lysis). For total protein lysate preparation, media were removed, and cells were washed twice withice-cold phosphate-buffered saline containing complete protease and PhosSTOP phosphatase inhibitor cocktail tablets (Roche Applied Science, Mannheim, Germany) and 1 mM Na3VO4. Lysis buffer (1% Triton X-100, 50 mM HEPES [pH 7.4],150 mM NaCl, 1.5 mM MgCl2, 1 mM EGTA, 100 mM NaF, 10 mM NaPPi, 10% glycerol,1 mM PMSF, 1 mM Na3VO4, and 10 μg/mL aprotinin). Samples were vortexed frequently on ice and then centrifuged. Cleared supernatants were collected and the protein was quantified using a BCA kit (Pierce Biotechnology) (5).

Western blot analysis

Western blot analysis was performed using SDS-PAGE followed by transfer to nitrocellulose membrane using the BioRad Gel system. Membranes were incubated in the following primary antibodies (1:1000) overnight: Chk1 (CST), pChk1 (Ser296; CST), γH2AX (S139) (CST), and cleaved caspase 3 (CST). Secondary antibodies were purchased from BioRad, detected using the Li-CorOdyssey-499 Imager, and image-captured and quantitated using Image Studio Version 2.1 software.

Establishment of flank xenografts and studies in nude mice

The mouse SCLC cell line was derived from tumors isolated from *Trp53/p130/Rb1* conditional knockout mice (mTmG cell line) (4). The H69/CR cell line is a cisplatin-resistant cell line

derived from the parental H69 cell line. H69/CR cells were grown in the absence of cisplatin for 4 weeks prior to injection into mice (6). For subcutaneous injections, 0.5×10^6 mouse SCLC (mTmG) and human SCLC (H69, H69/CR) cells were injected into one flank of each mouse with Matrigel (1:1, BD Biosciences).

Tumor growth assessment

Flank xenografts were established as described above. Tumors were evaluated twice weekly for the duration of the study. Nude mice with similar-sized tumors were identified. The length and width of tumors were measured manually with handheld slide calipers, and body weights of mice were measured using a bench top weighing scale. Tumor volume and body weights were measured on all mice three times per week and calculated ($\text{width}^2 \times \text{length} \times 0.4$). Once the average tumor size was in the range of 120-150 mm^3, mice were randomized into dosing groups using stratified sampling by assigning three animals per group for short-term reverse-phase protein array analysis and nine animals per group for long-term treatment. The randomization process ensured that the average tumor volume for each dosing group was approximately equal at the beginning of the study and mice with differing tumor volumes were evenly distributed among the groups. Dosing schedules and duration varied depending on the study. Mice were weighed and tumors were measured three times per week for the duration of the study, and a decrease in body weight >15% was considered indicative of a toxic dose. The Student *t* test was used to determine statistical significance between compound- and vehicle-treated groups.

Reverse-phase protein array (RPPA)

RPPAs were printed from lysates as previously described (7). The quality of the antibodies and validated by western blots and correlation of protein levels in previous RPPA experiments were

determined, as previously described (7). The RPPA samples were analyzed as described before (1)

Immunofluorescence

Immunofluorescence was performed using paraffin-embedded tumor sections (4 μm). Briefly, slides were deparaffinized and rehydrated with phosphate-buffered saline. For antigen unmasking, sections were boiled in 0.01M citrate buffer for 20 minutes. Nonspecific binding was blocked with Protein Block Serum-Free Ready-to-Use (DAKO) for 30 minutes at room temperature. Slides were then incubated with the primary antibodies (phospho-γH2AX, phospho-Histone H3) in 10% donkey serum in phosphate-buffered saline with Tween 20 (PBST) overnight at 4°C, washed, and incubated with Alexa-fluor conjugated secondary antibodies (1:600; Molecular Probes) for 45 minutes. Slides were counterstained with DAPI and cover-slipped with Slowfade Gold Antifade Reagent (Life Technologies).

SUPPLEMENTARY REFERENCES

1. Byers LA, Wang J, Nilsson MB, Fujimoto J, Saintigny P, Yordy J, *et al*. Proteomic profiling identifies dysregulated pathways in small cell lung cancer and novel therapeutic targets including PARP1. Cancer discovery **2012**;2:798-811
2. Johnson FM, Saigal B, Talpaz M, Donato NJ. Dasatinib (BMS-354825) tyrosine kinase inhibitor suppresses invasion and induces cell cycle arrest and apoptosis of head and neck squamous cell carcinoma and non-small cell lung cancer cells. Clinical cancer research : an official journal of the American Association for Cancer Research **2005**;11:6924-32
3. Jahchan NS, Dudley JT, Mazur PK, Flores N, Yang D, Palmerton A, *et al*. A drug repositioning approach identifies tricyclic antidepressants as inhibitors of small cell lung cancer and other neuroendocrine tumors. Cancer discovery **2013**;3:1364-77
4. Schaffer BE, Park KS, Yiu G, Conklin JF, Lin C, Burkhart DL, *et al*. Loss of p130 accelerates tumor development in a mouse model for human small-cell lung carcinoma. Cancer research **2010**;70:3877-83
5. Tibes R, Qiu Y, Lu Y, Hennessy B, Andreeff M, Mills GB, *et al*. Reverse phase protein array: validation of a novel proteomic technology and utility for analysis of primary leukemia specimens and hematopoietic stem cells. Molecular cancer therapeutics **2006**;5:2512-21
6. Heike Y, Takahashi M, Ohira T, Arioka H, Funayama Y, Nishio K, *et al*. In vivo screening models of cisplatin-resistant human lung cancer cell lines using SCID mice. Cancer chemotherapy and pharmacology **1995**;35:200-4
7. Byers LA, Sen B, Saigal B, Diao L, Wang J, Nanjundan M, *et al*. Reciprocal regulation of c-Src and STAT3 in non-small cell lung cancer. Clinical cancer research : an official journal of the American Association for Cancer Research **2009**;15:6852-61